such as calculi and teeth. We investigate ablation mechanisms of the lasers to achieve higher ablation effect for hard tissues.

2. Experiment and Discussion

We used an experimental setup shown in Fig. 1 to irradiate a hard tissue model with the two different lasers light. Ho:YAG (λ=2.1 μm) and Er:YAG (λ=2.94 μm) laser lights are combined by using a dichroic mirror and the laser beam is focused by a f=100 mm CaF_2 lens on the input end of a short hollow-fiber tip (100 mm in length) employed as a coupling optics. A hollow optical fiber with an inner diameter of 0.7 mm is butt-coupled to the short fiber that has the same diameter. The hollow fiber is coated with silver and cyclic-olefin polymer (COP) thin film on the inside and the thickness of COP is 0.3 μm so that the transmission losses for both of Er:YAG and Ho:YAG lasers are reduced by interference effect of the polymer film that acts as a reflection enhancement coating. The transmission losses of the hollow optical fiber used in the experiment are 1.0 dB for Ho:YAG and 0.5 dB for Er:YAG laser light.

The distal end of the hollow optical fiber is capped to keep the inside of fiber from vapor and debris of the ablated tissues. We used silica glass caps with a half ball shape. The focusing effect of the lens-shaped cap enables highly efficient ablation owing to the high energy intensity at the focal spot. The focal length of the cap is 1.0 mm from the end surface and the insertion loss is around 15%.

The emission timing and repetition rates of the pulses of the two lasers are controlled by an external trigger source and a delay line. To evaluate the ablation capabilities, we radiated lasers onto human teeth and alumina (Al_2O_3) ceramic balls used as a hard tissue model. We observed the ablation phenomenon by using an ultra-high-speed camera that has a capture speed of 50,000 frame/sec to investigate the ablation mechanism.

Firstly, we measured the depths and widths of ablated holes on alumina balls. We used alumina balls which are 4 to 6 mm in diameter and they had been soaked in water more than over night prior to the experiment.

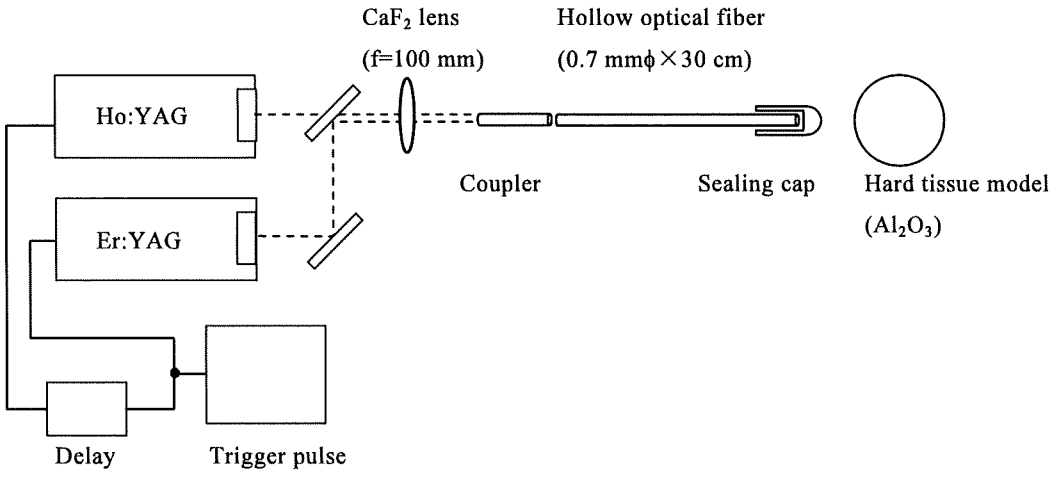

Fig. 1 Experimental setup with dual-wavelength laser

The pulse energies used in the experiment are 200 mJ and the pulse widths are 250 μs at the repetition rates of 3 Hz. The measured depths and widths as a function of pulse number are shown in Fig. 2 and cutting sections of ablated holes after 30 pulses are shown in Fig. 3.

It was found from the results in Fig. 2 that the widths are comparable for the both lasers and that, in contrast, the depths show clearly different appearances between the two lasers. When irradiated with the Ho:YAG, the depth saturated at large pulse numbers. This is because the energy density of the laser beam is getting lower than the ablation threshold of hard tissues when the beam spreads due to focusing effect of the lens cap. This happens in lower energy density for the Ho:YAG laser because of the lower absorption coefficient in water. For the Er:YAG, the depth increased linearly with the pulse shots because of the higher absorption coefficient in water.

Next we tested the ablation effect of the two lasers when they are simultaneously radiated. We change the delay time between the two lasers and observed the effect on ablation of ceramic balls. The pulse energies are 100 mJ for the both lasers and we compared the ablation depths with those made by the Er:YAG alone with a pulse

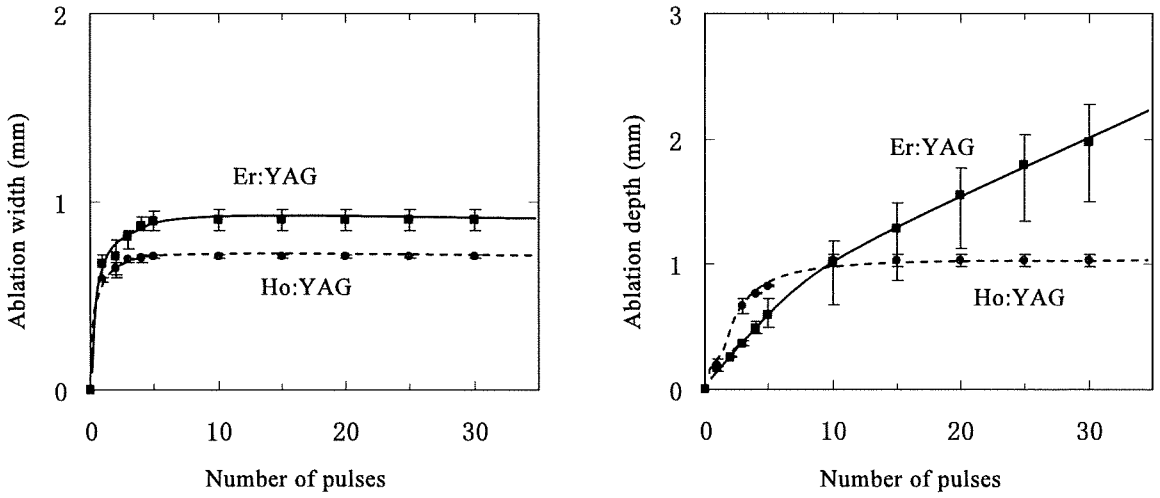

Fig. 2 Width and depth of ablated holes as a function of number of laser pulses

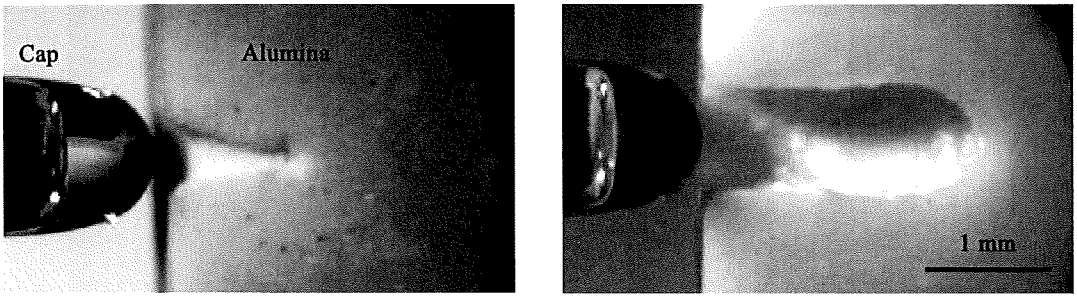

(a) Ho:YAG (b) Er:YAG

Fig. 3 Cutting sections of alumina balls after ablation of 30 pulses shot

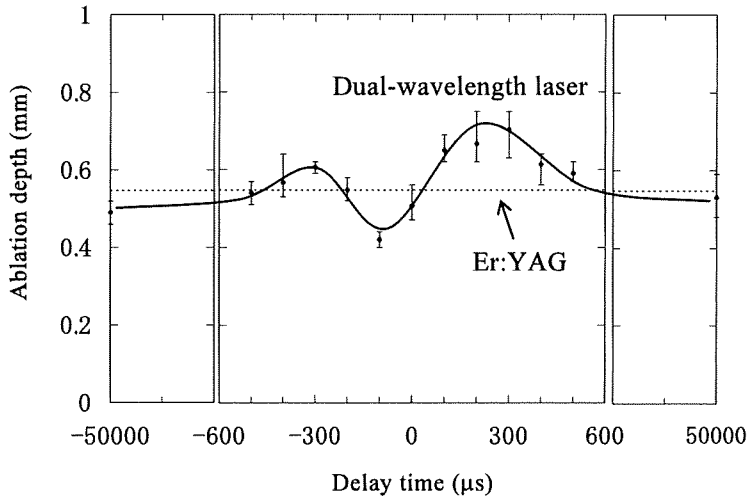

Fig. 4 Depths of ablated holes as a function of delay time

energy of 200 mJ. Figure 4 shows the depths of ablated holes as a function of delay time between the two lasers. The positive delay time means that we radiate the Ho:YAG before the Er:YAG. It is clear that the depths are highly dependent on the delay time and when irradiated with the delay time of $\pm$500 μs or smaller, depths drastically change with the delay. The largest depth is obtained at the delay time of 200-300 μs and obtained depth is 40% larger than that generated by the sole radiation of the Er:YAG laser.

To investigate the ablation mechanism of dual laser radiation, we observed the ablation phenomenon by using an ultra-high-speed camera. Alumina balls were irradiated with laser pulses and the moment of ablation at the surface was recorded at 50,000 frame/sec of capture speed. Figures 5 (a) and (b) show the ablation phenomenon with (a) Er:YAG and (b) Ho:YAG lasers alone and (c) is the moment of an Er:YAG pulse shot after

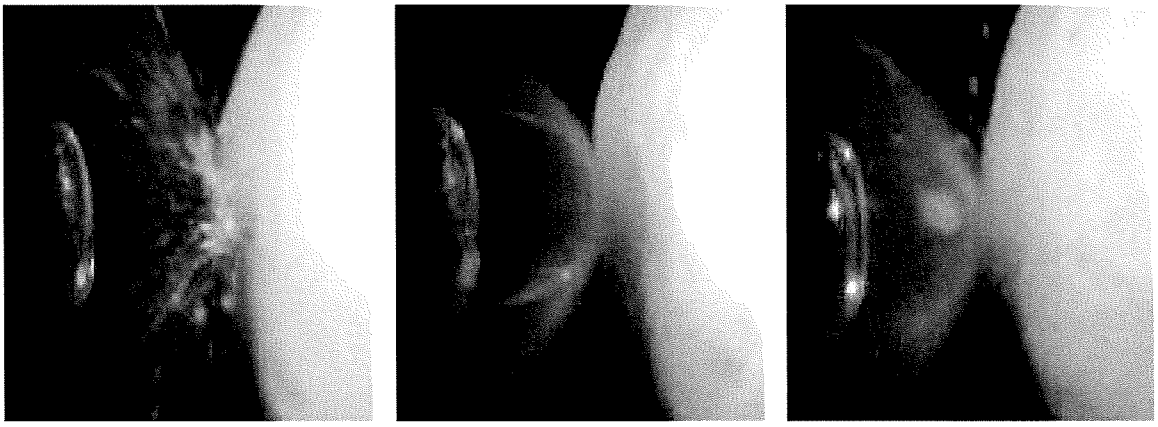

(a) Ho:YAG (b) Er:YAG (c) Ho:YAG and Er:YAG with a delay time of 200 μs

Fig. 5 Moment of ablation with Ho:YAG and Er:YAG lasers

a Ho:YAG with a delay time of 200 μs. When irradiated with Er:YAG laser light, powdery dust are scattered from the surface immediately after laser radiation. This is because the laser energy is absorbed in very surface of the ball. On the other hand, for the Ho:YAG laser, relatively large debris are sputtered. The laser beam penetrates into the ball and an explosive ablation occurred from the inside.

When an Er:YAG pulse is emitted after a Ho:YAG pulse (Fig. 5 (c)), large fragments were scattered. The Ho:YAG pulse that was radiated beforehand is absorbed and generates the heat. This causes decrease of absorption coefficient of water [5] and, as a result, Er:YAG laser beam can penetrates into the ball. In contrast, when a Ho:YAG pulse was shot after an Er:YAG, powdery dust were generated by Er:YAG and, after that, small debris were slightly sputtered from the surface. This is because the powdery dust scattered the most of the laser energy of delayed Ho:YAG pulse. As a result, the smallest depth was obtained in this case.

Next, we observed the heat generation during ablation of the alumina balls by using a thermographic camera. Figure 6 shows the thermal images of cutting sections of balls soon after laser radiation. When irradiated with Er:YAG laser, most of the pulse energy changed into the heat and stayed at the surface. In contrast, with the Ho:YAG laser, the energy penetrated deeper and therefore the induced heat diffused in a large area. This result comes from the difference of absorption coefficients and this is one of the reasons why the ablation with Ho:YAG occurred from the inside as shown in Fig. 5(a). At the optimum condition in Fig. 4 where the Er:YAG is emitted after Ho:YAG with a delay time of 200 μs, the heat was generated in deeper area before the Er:YAG pulse shot. This causes decrease of absorption coefficient of water and the Er:YAG laser beam penetrates deeper into the ball. Thermal lens effect may give an effect on deeper penetration as well.

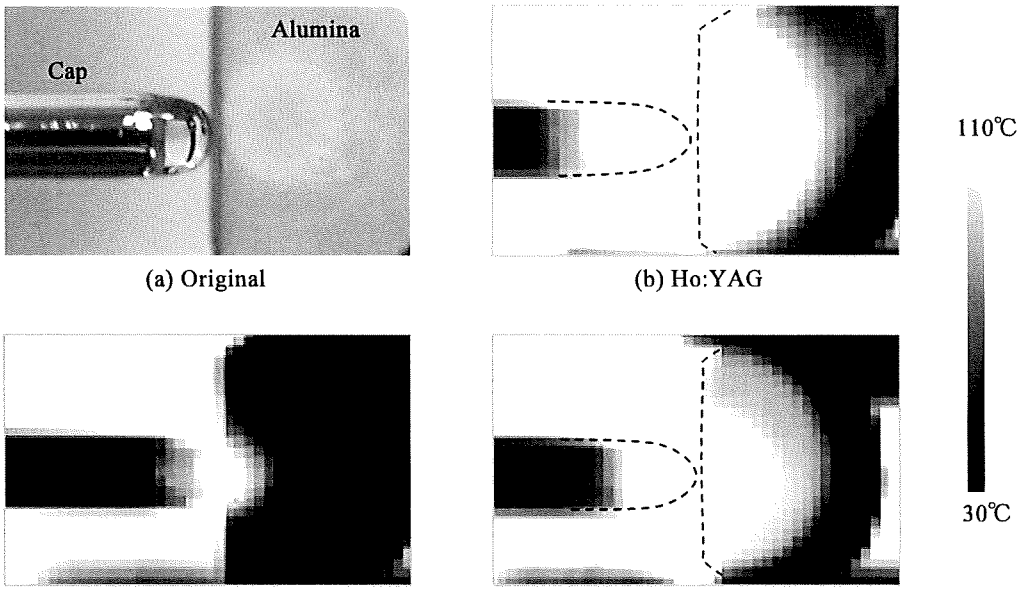

(a) Original (b) Ho:YAG

(c) Er:YAG (d) Ho:YAG and Er:YAG with a delay time of 200 μs

Fig. 6 Thermal images of cutting sections of balls after laser pulse

We also applied dual-wavelength laser radiation on human teeth. We sliced human tooth to the thin pieces with a thickness of 0.3 mm and radiated laser pulses on them. Figure 7 shows the cutting section of human tooth after laser irradiation of 5 pulses with a repetition rate of 3 Hz. When irradiated with two lasers, we obtained 15% larger depth than irradiated with Er:YAG only. On the teeth samples, we observed ablation effect that is similar to the ones for alumina balls and at the optimum condition described above, we obtained deep and sharp ablation holes on the teeth.

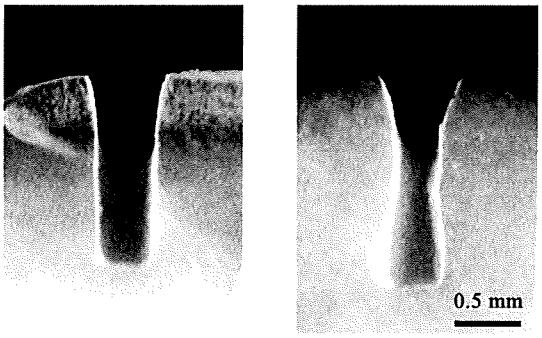

(a) Er:YAG (200 mJ) (b) Ho:YAG (100 mJ) and Er:YAG(100 mJ, 200 μs delay)

Fig. 7 Cutting section of human dentin after laser irradiation

3. Conclusion

Laser ablation experiments on hard tissues are performed by using a combined beam of Ho:YAG and Er:YAG laser light. An alumina ball is used as a hard-tissue model and ablation phenomenon are observed by an ultra-high-speed camera. The results show that the two lasers give different ablation effects due to different absorption coefficient in water contained in the tissues. When the two lasers are combined and the sample is irradiated with them, we observed that ablation capabilities are highly dependent on the delay time between two lasers and when Er:YAG laser was radiated after Ho:YAG with a delay time of 200 μs, 40% higher depth of ablated hole is made. We suppose that the Ho:YAG pulse induces heat and this causes decrease of absorption coefficient of water. And therefore, Er:YAG laser beam can penetrates deeper from the surface.

References

1. A. Aoki, et al., "Comparison between Er:YAG laser and Conventional Technique for Root Caries Treatment in vitro," J. Dent. Res., **77**, 1404-1414 (1998)
2. M. K. Yiu, et al., "Clinical Experience With Holmium:YAG Laser Lithotripsy of Ureteral Calculi," Lasers Surg. Med., **19**, 103-106 (1996)
3. H. Lee, et al., "Urinary calculus fragmentation during Ho:YAG and Er:YAG lithotripsy," Lasers Surg. Med., **38**, 39-51 (2006)
4. K. F. Chan, et al., "Free Electron Laser Ablation of Calculi: An Experimental Study," IEEE J. Quantum Electron., **7**, 1022-1033 (2001)
5. K. L. Vodopyanov, "Saturation studies of H_2O and HDO near 3400 cm-1 using intense picosecond laser pulses," J. Chem. Phys., vol. **94**, no. 8, pp. 5389-5393 (1991)

Fabrication of hollow optical fiber with a vitreous film for CO_2 laser light delivery

Katsumasa Iwai[1)], Mitsunobu Miyagi[1), 2)], Yi-Wei Shi[3),*], Xiao-Song Zhu[3)], Yuji Matsuura[4)]

1) Sendai National College of Technology,
4-16-1 Ayashi-chuo, Aoba-ku, Sendai, 989-3128, Japan.
2) Miyagi National College of Technology,
48 Nodayama, Shiote, Medeshima, Natori 981-1239, Japan
3) Department of Communication Science and Engineering, Fudan University,
220 Handan road, Shanghai 200433, China. * Email: ywshi@fudan.edu.cn
4) Graduate School of Engineering, Tohoku University,
Aramaki Aoba, Aoba-ku, Sendai 980-8579, Japan.

Abstract

Vitreous film based on the structural unit R_2SiO, where R is an organic group, is newly used as the reflection layer in the hollow optical fiber for CO_2 laser delivery. A smooth vitreous film is formed at room temperature by using the liquid-phase coating technique. The vitreous film-coated silver hollow optical fibers achieve low-loss property for lasers in the infrared regions by properly selecting fabrication conditions. A hollow fiber with thicker vitreous film designed for CO_2 laser light showed acceptable loss as an output tip. It is shown that the hollow tip is of high durability to withstand several cycles of autoclave sterilization.

Keywords: hollow fiber, CO_2 laser, infrared laser.

1. Introduction

CO_2 laser radiating at the wavelength of 10.6 μm has been used as the energy source of laser scalpel because CO_2 laser light has a high incision capacity as well as coagulation effect. Therefore CO_2 laser has become one of the widely used medical lasers in clinician. As the transmission media for infrared laser light, hollow optical fiber [1-3] is one of the commonly used infrared fibers. We have been doing research on dielectric coated metallic hollow optical fiber for various industrial and

Optical Fibers and Sensors for Medical Diagnostics and Treatment Applications IX, edited by Israel Gannot,
Proc. of SPIE Vol. 7173, 71730Q · © 2009 SPIE · CCC code: 1605-7422/09/$18 · doi: 10.1117/12.807602

medical lasers [4].

For the dielectric coated metallic hollow optical fiber, silver is normally used as the metallic layer, because silver has a high reflection rate in the infrared wavelength region. Cyclic olefin polymer (COP) [3] is one of the normally used dielectric materials. COP-coated silver hollow optical fibers obtained low-loss property not only in the infrared region but also in the visible region. Simultaneous delivery for infrared and pilot laser beam is possible by using this kind of hollow fiber. In medical laser treatment through hollow optical fiber, CO_2 laser irradiated the diseased tissue with the distal end of the fiber contacting the target. Therefore durability of the hollow fiber is important. Hollow optical fiber tip is often sterilized by an autoclave treatment for medical applications after irradiation. COP-coated hollow optical fiber has an obvious deterioration after the sterilization streatment. This can be cause by the somewhat weak adhesion between COP and silver layer.

In this paper, we report the inorganic material coated on silver hollow optical fiber for CO_2 laser delivery. Normally, inorganic materials have higher temperature capability and stronger adhesion to silver layer. The inorganic material is a vitreous layer that is formed by using an OC-300 [5, 6] solution. A smooth hardened film can be formed on the silver layer with the treatment of hardener solution at room temperature by using liquid-phase coating technique. The OC-300 coated hollow optical fiber shows stronger durability in medical application.

2. Inorganic coating material for hollow fiber

We tried to use an inorganic material OC-300 [5, 6] as the dielectric film. OC-300 is a semi-inorganic polymer which is originally developed as a protecting painting for outside wall of buildings or ground floor. It is a commercially available product, which is sold in a two-solution set. OC-300 is the trade name of the coating material. It is a semi-inorganic polymer based on the structural unit R_2SiO, where R is an organic group. The material is characterized by wide-range thermal stability, water repellence, and physiological inertness.

In the two-solution set, one is the main paint solution and the other is a hardener solution. When the main solution is mixed with the hardener solution, a hardened vitreous film can be formed with the catalysis of water in the air. Figure 1 shows the procedure of the vitreous film formation. The film has properties similar to that of a SiO_2 film.

In this research, the mixing rate of the main paint solution and the hardener was 10:1. The concentration of OC-300 solution is calculated by considering mixing ratio of the above solution and the paint thinner. The final solution is mixed by using a magnetic stirrer for about five minutes. And the solution is stored for a couple of hours to become stabilized before used in liquid-phase coating process. Comparing with the COP solution, the OC-300 solution has a lower viscosity.

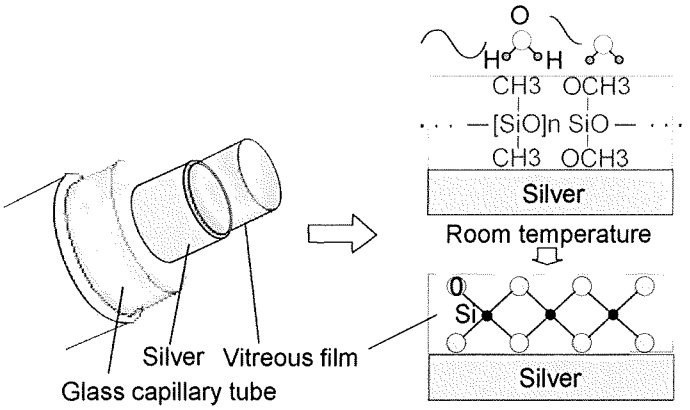

Figure 1. Structure of OC-300 coated silver hollow optical fiber

3. Fabrication and transmission property

We use chemical deposition method to plate silver layer on the glass capillary. The silver layer has a smoother surface when we pretreated the inner surface with a $SnCl_2$ solution. This is a guarantee for high performance hollow optical fiber. Details of the process had been described elsewhere [3].

The dielectric layer is important for a low-loss fiber. Liquid-phase coating method [7] was used to coat an OC-300 layer. The merit of using OC-300 as the dielectric layer is not only for its proper refractive index nearer to the optimum of 1.41 but also for the low temperature of film formation. This property gives great credit to a high flexible hollow fiber. As we have shown [8], the flexibility of a glass hollow fiber will deteriorate largely duo to high temperature curing process, while the process is often necessary in many dielectric film-coating techniques.

Thick film coating of OC-300 layer for CO_2 laser light transmission was proved to be possible. The viscosity of the mixed solution can be modified by changing the ratio of the two solutions. As we have known that high viscosity leads to thicker film in the liquid-phase coating technique. Relationship between OC-300 film thickness and the concentration of OC-300 solution is shown in Fig. 2. The OC-300-coated silver (OC300/Ag) hollow optical fiber is 10 cm long with 1 mm inner diameter. And the flowing speed of OC-300 solution is around 1.6 cm/min in the fabrication. After the liquid-phase coating, the fiber was treat at the room temperature with nitrogen gas flowing through the hollow core for 24 hour. The liquid-phase OC300 film was changed to a vitreous layer on the silver surface. As we have known, OC-300 solution with high concentration leads to a thicker OC-300 layer. For laser light in mid-infrared region, such as CO_2 laser radiating at 10.6 μm, a relatively thicker OC-300 film of about 1 μm is required. We note that the concentration of OC-300 solution is about 65 wt% in fabricating hollow optical fiber for CO_2 laser light.

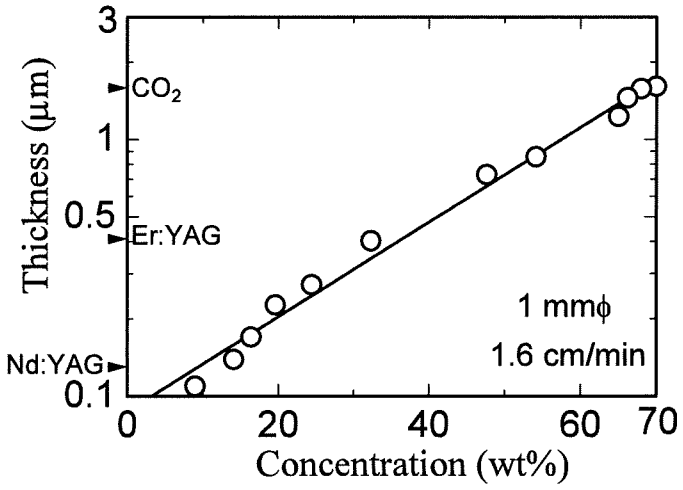

Figure 2. OC-300 film thickness as a function of the solution concentration. The flowing speed of OC-300 solution was around 1.6 cm/min and the fiber is 10 cm long with 1 mm inner diameter.

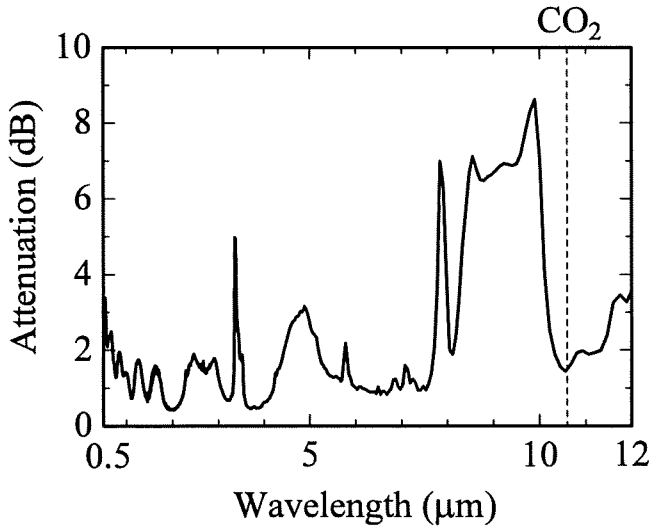

Figure 3. Loss spectrum of OC-300/Ag hollow fiber in the wavelength region from the visible to the mid-infrared. The fiber is 10 cm long with 1 mm inner diameter.

Figure 3 shows the loss spectrum of OC-300/Ag hollow fiber in the wavelength region from the visible to the mid-infrared. The fiber is 10 cm long with 1 mm inner diameter. According to the interference peaks in the visible and near infrared regions, the film thickness of the vitreous layer is calculated as 1.2 μm. The absorption peak at the wavelength of 3.5 μm is caused by impurities that contains -CH band in the main solution. The wide loss peak in the wavelength region from 8 μm to 10 μm comes from the absorption of Si-O band in the vitreous film over the silver layer. The interference

peaks in the visible and near infrared wavelength region show a smooth dielectric layer on the silver surface. The fiber attains low loss at the wavelength of 10.6 μm for CO_2 laser light.

4. Durability for sterilization treatment

Figure 4 shows the transmission property of OC-300/Ag hollow fiber for CO_2 laser light after sterilization cycles by using an autoclave device. The autoclave device is standard sterilization equipment for medical applications.

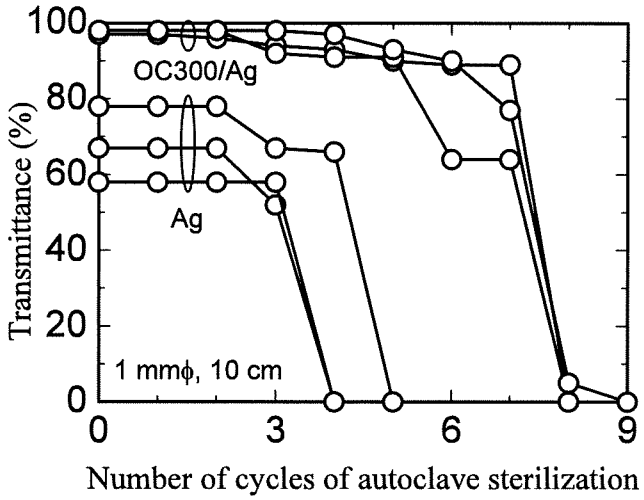

Figure 4. Transmittance for CO_2 laser light of two kinds of hollow fiber after autoclave sterilization treatment. Fibers are 10 cm long with 1 mm inner diameter.

The output of CO_2 laser used in the measurement was set as follows. The input power was 0.15 W. The treatment condition of the autoclave is 135°C for 25 minutes per cycle. The humidity and the pressure in the sample chamber of the autoclave are 100% and 2 atmospheric pressure, respectively. Transmission properties of a silver coated hollow optical fiber are also added for comparison. Data came from around three samples for each kind of hollow fiber. After each autoclave treatment cycle, samples are dried at room temperature for 30 minutes while nitrogen gas flowing through the hollow core at a lowing flowing rate of 100 ml/min. Then the next measurement and sterilization cycle was conducted. This drying process was taken to evaporate the water remained inside of the hollow core of the fiber during autoclave treatment. Without the drying process, damages occur on the dielectric layer of the hollow optical fiber when CO_2 laser light is delivered. Because water on the inner surface absorbs the CO_2 laser light energy and instant temperature is as high as several hundred degrees centigrade. Vitreous film or even the silver layer can be broken due to the high temperature.

We note in fig. 4 that Ag only hollow optical fibers have low transmittance and obvious deterioration after autoclave treatment. Temperature and humidity in the autoclave caused secession between silver layer and the glass surface of hollow optical fiber. After several treatment cycles the silver film deteriorated largely. On the other hand, OC300/Ag hollow optical fibers obtain obviously higher transmittance for CO_2 laser light and the property was stable in several treatment circles. The film thickness of the vitreous layer is 1.2 μm. For the 10 cm long tip, with an inner diameter 1 mm, its loss is less than 0.5 dB. It is acceptable for most medical device used as an output tip. This means that OC-300 adheres strongly on the silver surface and protect silver layer against humidity damage under high pressure.

5. Conclusion

We used an inorganic material as the reflection layer in hollow optical fiber for CO_2 laser light delivery. The vitreous film can be easily formed at room temperature by using liquid-phase coating method. A thicker OC-300 film with 1.2 μm thickness was successfully coated and the fiber attained low-loss property for CO_2 laser light radiating at the wavelength of 10.6 μm. The loss for the 1 mm inner diameter, 10 cm length OC300/Ag hollow fiber was 0.2 dB. The OC-300 coated hollow optical fibers are of low-loss property and high durability. It can be used in a relatively harsh industrial environment or used as a probe in medical field for repeating utilization in medical applications.

Acknowledgements

This research is supported by the Ministry of Education, Science, Sports and Culture of Japan through a Grant-in-Aid for Scientific Research (B) (20360164) and (B) (19760240) 2008 and Health and Labor Science Research Grants (H20-nano-young-010) 2008, as well as by the National Nature Science Foundation of China (60608013) and by the Scientific Research Foundation for the Returned Overseas Chinese Scholars, State Education Ministry.

References

1. I. Gannot, S. Schrunder, J. Dror, A. Inberg, T. Ertl, J. Tschepe, G. J. Muller, and N. Croitoru, "Flexible waveguides for Er-YAG laser radiation delivery," IEEE Trans. Biomedical Eng. **42**, 967-972 (1995).
2. R. K. Nubling and J. A. Harrington, "Hollow waveguide delivery system for high-power,

industrial CO_2 lasers," Appl. Opt. **35**, 372-380 (1996).

3. Y. W. Shi, Y. Wang, Y. Abe, Y. Matsuura, M. Miyagi, S. Sato, M. Taniwaki, and H. Uyama, "Cyclic olefin polymer-coated silver hollow glass waveguides for the infrared," Appl. Opt. **37**, 7758-7762 (1998).
4. M. Miyagi and S. Kawakami, "Design theory of dielectric-coated circular metallic waveguides for infrared transmission," IEEE J. Lightwave Technol. **LT-2**, 116-126 (1984).
5. K. Iwai, Y. W. Shi, M. Miyagi, X. S. Zhu, and Y. Matsuura, "Hollow infrared fiber with an inorganic inner coating layer with high durability," Proc. of SPIE **6433**, 64330L-1-64330L-7 (2007).
6. K. Iwai, M. Miyagi, Y. W. Shi, X. S. Zhu, and Y. Matsuura, "Infrared hollow fiber with a vitreous film as the dielectric inner coating layer," Opt. Lett. **32**, 3420-3422 (2007).
7. K. Iwai, Y. W. Shi, M. Miyagi, and Y. Matsuura, "Improved coating method for uniform polymer layer in infrared hollow fiber," Opt. & Laser Technol. **39**, 1528-1531 (2007).
8. Y. W. Shi, K. Ito, L. Ma, T. Yoshida, Y. Matsuura, and M. Miyagi, "Fabrication of a polymer-coated silver hollow optical fiber with high performance," Appl. Opt. **45**, 6736-6740 (2006).

2D09

内径 50 μm 赤外伝送用銀中空ファイバの製作

阿部 直雪*, 庄子 健太郎**, 岩井 克全*, 宮城 光信*, ***, 石 芸尉****
*仙台電波工業高等専門学校, **東北工業大学, ***宮城工業高等専門学校, ****復旦大学

1. はじめに

歯科根管治療等の低侵襲治療に、中空ファイバの導入を図り、内径 100 μm 以下の超細径銀中空ファイバの製作を行ってきた [1, 2]。本研究では、効率よい低侵襲治療を行うために、より細径な内径 50 μm 銀中空ファイバの製作を試みた。

2. 銀中空ファイバの製作と評価

図 1 に、銀鏡反応を用いた内径 50 μm 銀中空ファイバの製作装置を示す。ファイバ内径が細いと銀鏡反応溶液の流量が低下し、粗い銀膜が成膜される。そこで、ガラスキャピラリチューブ (内径 50 μm、外径 150 μm、長さ 50 cm)を 300 本束ねたバンドルを製作し、断面積を大きくすることで、流量の増加を試みた。

図 2 に、ガラスキャピラリチューブの本数に対する蒸留水の流量を示す。ガラスキャピラリチューブを 300 本束ねたバンドル 1 本では、流量 0.5 ml/min であった。バンドル 16 本(ガラスキャピラリチューブ総数 4800 本)を並列接続することで、流量 8.6 ml/min と流量を大幅に増加することができた。

銀鏡反応の前処理液として $SnCl_2$ 溶液を用い、真空ポンプにより、銀液と還元液を吸い上げ、ミキサー部で混合させた溶液をバンドルに流し、内面に銀を成膜する。銀粒子の成長は溶液温度に依存し、温度が高いほど速く成長するため、低い溶液温度 16℃とした。銀鏡反応時間 12 分 30 秒とし、後洗浄 (蒸留水 3 分間、エタノール 1 分間流す)を行い、その後、窒素を流しながら 60℃の加熱乾燥を 30 分間行った。

図 3 に内径 50 μm 銀中空ファイバ (長さ 10 cm、10 本)の可視-近赤外の損失波長スペクトル (FWHM10.6 ° のガウスビームで励振)を示す。ファイバの損失値に、ばらつきがあることが分かる。これは、バンドル形成の際、端面を揃える事が困難であり、溶液の流れ易さがファイバで異なってしまったためと思われる。波長 1 μm において、最も低損失なファイバは、12.5 dB となった。

3. まとめ

内径 50 μm 銀中空ファイバの製作を試みた。銀鏡反応を用いた内径 50 μm 銀中空ファイバの製作は、ガラスキャピラリチューブを、バンドルにし並列接続することで、可能なことを確認した。

参考文献

1) 岩井、志賀、宮城、石、松浦、信学ソ大、C-3-32 (2007).
2) 岩井、板垣、安藤、宮城、石、松浦、電子情報通信学会総合大会、B-13-2 (2009).

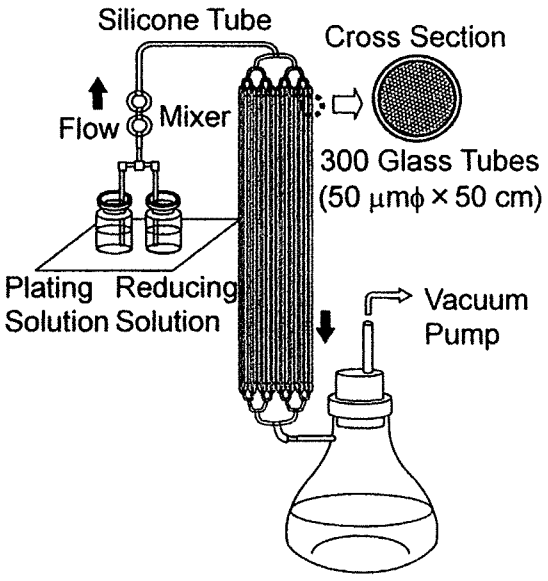

図 1 超細径銀中空ファイバ製作装置

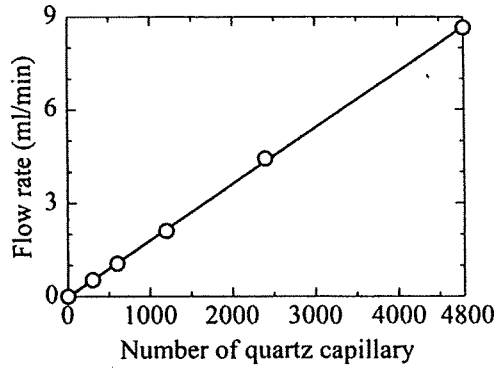

図 2 ガラスキャピラリ(内径 50 μm、長さ 50 cm)のバンドル数に対する蒸留水の流量

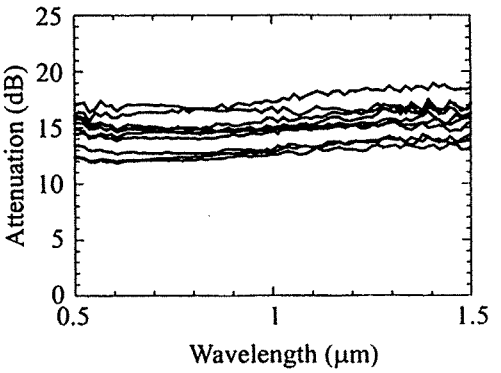

図 3 銀中空ファイバ(内径 50 μm、長さ 10 cm)の可視-近赤外の損失波長スペクトル(FWHM10.6 °のガウスビームで励振)

2D05

充填コーティング法を用いた AgI 内装銀クラッド SUS 管先端チップの製作

岩井 克全*, 高久 裕之*, 宮城 光信*, **, 石山純一**, 本郷 晃史***, 石 芸尉****
*仙台電波工業高等専門学校, **宮城工業高等専門学校, ***日立電線, ****復旦大学

1. はじめに

医療現場の感染対策として，滅菌処理対応の赤外レーザ用先端チップが求められているが，従来の光学膜内装銀中空ファイバの耐久性では十分でない。そこで，耐久性に優れた銀クラッド SUS 管と，光学膜にヨウ化銀(AgI)層[1, 2, 3]を選択し，ヨウ素廃液を大幅に低減できる簡易な充填コーティング法を用い先端チップの製作を行う。

2. 充填コーティング法を用いた AgI 形成法

銀クラッド SUS 管(内径 0.75 mm, 外径 1.2 mm, 長さ 28 cm)は，内側にメカニカル研磨した厚さ 100 μm 程度の銀層とその外側はステンレスの構造となっている。ヨウ素(粒)の溶剤にシクロヘキサンを用い，超音波(40 kHz)照射と撹拌を 10 分程度行い，ヨウ素液を製作した。図 1 に AgI 膜のコーティング装置を示す。シリンジポンプを用いて，銀クラッド管内にヨウ素液を充填し，AgI 膜の形成後，ヨウ素液の排出を行う。ヨウ素液を充填するまでの時間は約 4 秒である。

3. AgI 内装銀クラッド SUS 管先端チップの試作

製作した AgI 内装銀クラッド SUS 管先端チップの波長損失スペクトルを測定し，干渉ピークから AgI 膜厚の推定を行った。図 2 にヨウ素液の充填時間と AgI 膜厚の関係を示す。Er:YAG レーザ用の AgI の最適膜厚 0.22 μm を破線で示す。最適膜厚の形成条件は，濃度 0.5 %のヨウ素溶液を用いて，充填時間 60 秒であることが分った。充填時間を長くすると，膜厚が増加するが，長くし過ぎると膜厚の増加が少なくなる傾向にあることが分った。これはヨウ素液の濃度が薄くなることと，形成された AgI 膜により反応が抑えられたためと思われる。

次に CO_2 レーザ光伝送に最適な AgI 膜厚の形成条件を求める。図 3 にコーティング処理の回数と AgI 膜厚の関係を示す。但し，ヨウ素液の濃度は 1%を用いた。CO_2 レーザ光伝送に最適な膜厚 0.88 μm を破線で示す。充填時間 240 秒間，コーティング処理 3 回で製作できることが分った。

4. まとめ

充填コーティング法を用いて AgI 内装銀クラッド SUS 管先端チップの試作を行った。溶液の充填時間，処理回数に対する AgI の成膜特性を明らかにした。

参考文献
1) M. Alaluf et al., J. Appl. Phys. **72**, 3878-3883 (1992).
2) J. A. Harrington et al., IEEE J. Quantum Electron. **5**, 948-953 (1999).
3) Y. Matsuura et al., Appl. Opt. **35**, 5395-5397 (1996).

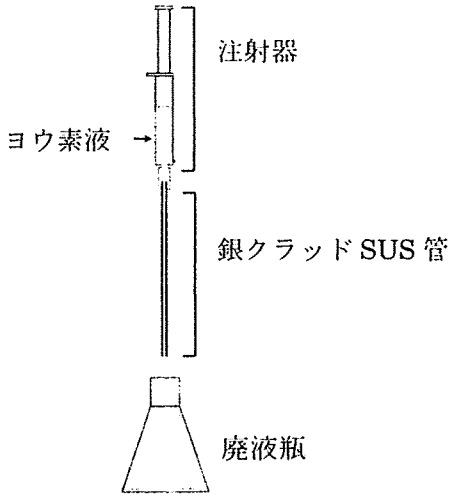

図 1　AgI 膜のコーティング装置

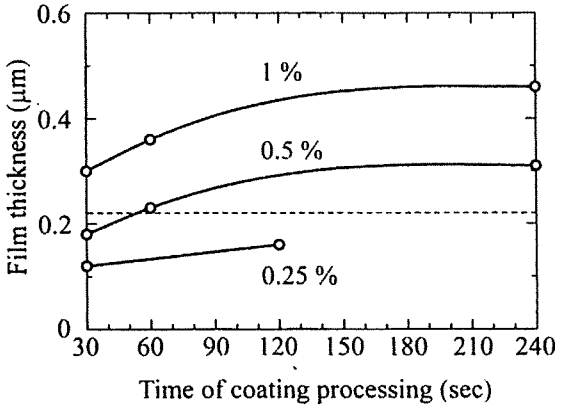

図 2　コーティング処理の充填時間に対する AgI 膜厚特性（図中の%はヨウ素濃度）

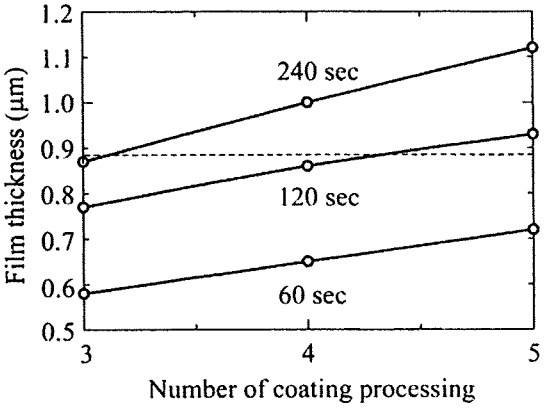

図 3　コーティング処理の回数と AgI 膜厚特性
但し，溶液濃度 1%、図中の sec は充填時間

銀クラッドステンレス管を用いたAgI/Ag中空ファイバの伝送特性

Transmission Properties of AgI/Ag Hollow Optical Fibers Based on Silver-Cladding-Stainless Pipe

岩井 克全[*1] 高久 裕之[*1] 宮城 光信[*1,2] 石山 純一[*2] 本郷 晃史[*3] 石 芸尉[*4]
Katsumasa Iwai Hiroyuki Takaku Mitsunobu Miyagi Jun-ichi Ishiyama Akihito Hongo Yi-Wei Shi

[*1] 仙台電波工業高等専門学校 [*2] 宮城工業高等専門学校 [*3] 日立電線 [*4] 復旦大学
Sendai National College of Tech. Miyagi National College of Tech. Hitachi Cable Ltd. Fudan Univ.

1. はじめに

筆者らは、これまでポリマー膜内装銀中空ガラスファイバの高機能化を行ってきた。審美治療のレーザプローブ等、CO_2 レーザ光の高エネルギー伝送用には、耐熱性、熱伝導を考慮すると、無機のヨウ化銀(AgI)膜 [1]を内装した金属製の中空ファイバが有効である。

本論文では、銀クラッドステンレス管を用いたヨウ化銀内装銀(AgI/Ag)中空ファイバの伝送特性について述べる。

2. AgI/Ag 中空ファイバの設計

図 1 に、銀(Ag)中空ファイバの内壁に、AgI 層を 1 層内装した時の HE_{11} モードの伝送損失を、AgI の膜厚に対し示した。ここで、伝送する CO_2 レーザ光の波長は 10.6 μm、AgI の屈折率は 2.1、 Ag の複素屈折率は 13.5−j75.3 としている。AgI の膜厚を適当に選択することで低損失な中空ファイバが得られ、AgI 層の最適膜厚 d は 0.89 μm と求められる。

図 2 に、CO_2 レーザ光に対し最適膜厚の AgI 層を形成した中空ファイバ (コア径 0.75 mm)における HE_{11} モードの理論的な損失波長特性を示す。明確な損失ピークがあり、このピークの位置は、内装誘電体の膜厚に依存するため、損失がピークとなる波長の測定により、内装 AgI の膜厚を推定することができる。

3. AgI 内装銀クラッドステンレス管の伝送特性

内径 0.75 mm、長さ 280 mm の銀クラッドステンレス管を用い、AgI/Ag 中空ファイバの製作を行った。銀クラッド層は機械的に研磨されており、100 μm 程度の厚さがある。AgI 層はヨウ素液を用い、液相法により製作している。

図 3 に、銀クラッドステンレス管を用いた AgI/Ag 中空ファイバの波長損失特性を示す。明確な損失ピークが現れており、銀クラッド内面に、均一な AgI 層を形成できていることを示している。最適膜厚に近い 0.91μm と最適値よりやや薄い 0.71μm の伝送損失は、波長 10.6μm において 1.1dB 程度と低損失になった。膜厚が厚いと粗さが大きく、損失も増加することから、最適膜厚より、やや薄い膜を形成すると低損失な中空ファイバが製作し易い。

4. まとめ

銀クラッドステンレス管を用いた AgI/Ag 中空ファイバの設計および製作したファイバの伝送特性の測定を行った。波長 10.6 μm で 1.1dB と、低損失なことを確認した。

参考文献

1) Y. Matsuura et al., Appl. Opt. 35, 5395-5397 (1996).

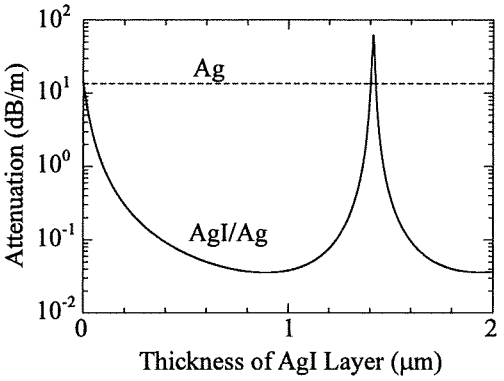

図 1 CO_2 レーザ光伝送における AgI 膜厚に対する HE_{11} モードの伝送損失
但し、中空コア径 0.75 mm、AgI の屈折率 2.1

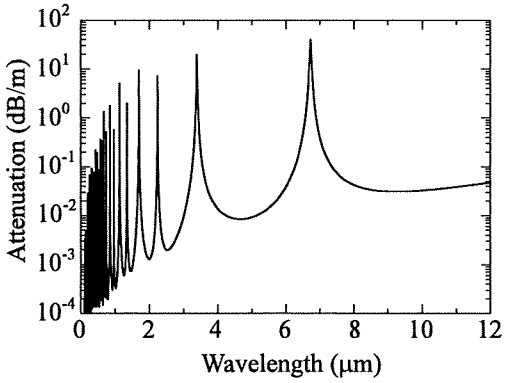

図 2 AgI 層を最適膜厚(d=0.89 μm)にしたときの HE_{11} モードの損失波長特性

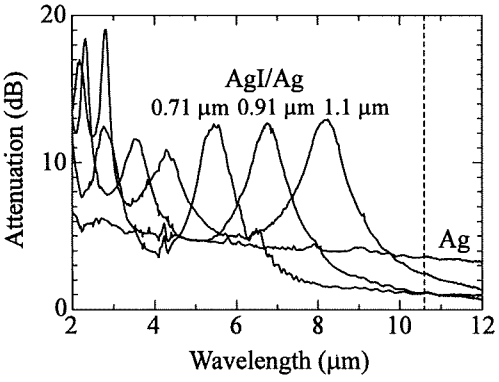

図 3 銀クラッドステンレス管を用いた AgI/Ag 中空ファイバ(内径 0.75 mm、長さ 280 mm)の損失波長特性
但し、図中の値は、AgI 膜厚